Catalysis Today 142 (2009) 227–233

Contents lists available at ScienceDirect

Catalysis Today

journal homepage: www.elsevier.com/locate/cattod

Liquid phase oxidation of dibenzothiophene with alumina-supported vanadium oxide catalysts: An alternative to deep desulfurization of diesel

H. Gómez-Bernal, L. Cedeño-Caero *, Aída Gutiérrez-Alejandre

Facultad de Química, Departamento de Ingeniería Química, Universidad Nacional Autónoma de México, México D.F. 04510, Mexico

ARTICLE INFO

Article history:
Available online 19 September 2008

Keywords:
Supported vanadium oxide catalysts
ODS
Liquid phase oxidation
Preparation method

ABSTRACT

Alumina-supported vanadium oxide catalysts were prepared by different methods as thermal spreading, incipient wetness impregnation of ammonium metavanadate and sol–gel synthesis of alkoxide precursors, with different vanadium loadings, in order to increase the performance in oxidative desulfurization (ODS) of dibenzothiophene. The catalysts were characterized by several techniques: X-ray diffraction, UV–vis DRS, Raman spectroscopy, FT-IR of adsorbed pivalonitrile, and TPR. As additional experimental techniques, SEM–EDX and N_2 adsorption–desorption were applied, to obtain elemental analyses and textural properties. Results evidenced the presence of different superficial V species, which depend on both vanadium loading and preparation method, while significant differences in ODS activity were observed due to the catalysts preparation method.

1. Introduction

Refiners worldwide are substantially reducing sulfur levels in transportation fuels in order to meet current and upcoming regulations imposed in various countries. Depending on locality, some gasoline and on-road diesel sulfur concentrations will need to be less than 30 ppm, versus levels that may exceed 500 ppm today. As with past fuel specification changes, refiners and technology providers are finding resourceful solutions to comply with new, more stringent fuel specifications [1,2]. Dibenzothiophene derivatives are the predominant sulfur species remaining after hydrodesulfurization [2]. Oxidative desulfurization (ODS) wherein dibenzothiophene derivatives are converted to their corresponding sulfone is an approach that is being actively pursued using a variety of different methodologies [3]. ODS is a current process and has been discussed recently in previous publications [4–12], where the oxidized sulfur compounds can be removed from the hydrocarbon phase by extraction or precipitation. The sulfones are highly polar compounds and are easily separated, during ODS process, from the fuel product by extraction [10]. In that study, the sulfones were obtained predominantly in the solvent phase, and activity profiles describe a consecutive process scheme, being the dibenzothiophenes (DBTs) extracted the intermediate "product"

$$DBTs_{(diesel)} \rightarrow DBTs_{(solvent)} \rightarrow Sulfone_{(solvent)}$$

Hence, liquid phase oxidation of sulfur compounds is the basis of the ODS process, since extraction step occurs rapidly and oxidation is the rate determining step.

Vanadium oxide has demonstrated to improve S-compounds oxidation, thus it has been used as active phase in our recent studies [10–12]. In these studies we evaluate vanadium-based catalysts with different supports [12], which show high activity for sulfur removal of actual Mexican diesel, and for a model diesel with N-compounds [11]. In order to improve the activity of these catalysts, this work evaluates different preparation methods of V_2O_5/Al_2O_3, concerning their catalytic performance in the liquid phase oxidation of dibenzothiophene, which is the basis of the ODS process.

2. Experimental

2.1. Catalyst preparation

VO_x/Al_2O_3 catalysts with various vanadium loadings were prepared by thermal spreading (TS), incipient wetness impregnation (IWI) and sol–gel (SG). Preparations by TS consisted in intensive mixing and manual milling of vanadium pentoxide

* Corresponding author. Tel.: +52 55 56225369; fax: +52 55 56225366.
E-mail address: caero@servidor.unam.mx (L. Cedeño-Caero).

0920-5861/$ – see front matter © 2008 Elsevier B.V. All rights reserved.
doi:10.1016/j.cattod.2008.08.018

(J.T. Baker) and γ-Al_2O_3 (Gilder). The solid mixtures were subsequently calcined at 500 °C during 8 h.

Other catalysts were prepared by IWI of Al_2O_3 with solutions of ammonium metavanadate (Sigma–Aldrich, 99%) dissolved in aqueous oxalic acid 2 M (Aldrich, 97%). After 12 h of aging, catalysts were dried at 100 °C during 24 h and calcined at 500 °C during 8 h.

Sol–gel catalysts were prepared by mixing, at 60 °C, vanadium (III) acetyl-acetonate ($V(acac)_3$; Aldrich, 97%) with 1 M solutions of aluminum *tri–sec*-butoxide (Aldrich, 97%) dissolved in 2-butanol (Fluka, 99.5%). After complete dissolution of $V(acac)_3$ was achieved, the mixture was cooled to room temperature and a stoichiometric amount of water (H_2O:$Al[OCH(CH_3)C_2H_5]_3$, 3:1) was added to perform hydrolysis. The obtained gels were dried at 120 °C during 24 h and consequently calcined at 500 °C during 5 h.

Catalysts labels are composed by a number that stands for the nominal percentage of V_2O_5 on alumina (VA), and the last two or three letters for the preparation method, i. e. 10VATS.

2.2. Catalyst characterization

Textural properties of the catalysts were obtained by N_2 adsorption–desorption isotherms of the samples, with a Tristar Micromeritics apparatus. Nitrogen physisorption isotherms were analyzed using the BJH and BET methods. Prior to the textural analysis, the samples were outgassed for 8 h in vacuum at 350 °C. Elemental composition was determined by SEM–EDX in a Jeol JSM-5900 LV microscope equipped with an energy dispersive X-ray (EDX) elemental analysis system. Catalysts were further characterized by: X-ray diffraction (XRD) using a Siemens D500 powder diffractometer with Cu Kα radiation. The FT-Raman spectra of catalysts were taken at ambient conditions in a Thermo-Nicolet Almega Dispersive Raman spectrometer with a resolution of 4 cm^{-1} and 500 scans per spectrum. A conventional temperature-programmed reduction (TPR) apparatus was used to study the reducibility of the catalysts. TPR was performed using a flow of H_2/Ar mixture (30% H_2, v/v, 25 cm^3/min) at atmospheric pressure, 0.25 g of sample and a heating rate of 10 °C/min from room temperature to 1000 °C. Diffuse reflectance spectra were collected with a Cary 500 Scan UV–vis–NIR Spectrophotometer at room temperature with a Halon white reflectance standard as baseline. Before the analysis, the samples were pretreated at 100 °C during 5 days in static air, except NH_4VO_3 due to its known decomposition into V_2O_5 and NH_3 at this or higher temperatures. This compound was only dried at room temperature with desiccant. IR spectra were performed on a Nicolet Magna 760 Fourier Transform Spectrometer with a resolution of 2 cm^{-1} and 300 scans. For IR experiments, wafers of pure catalyst were made and outgassed under high vacuum in a special IR cell at 450 °C during 1 h to physically remove adsorbed impurities from the catalyst sample. After that, the sample was cooled up to room temperature and then 12 Torr of pivalonitrile (PN; Aldrich, 98%) were introduced and the corresponding spectrum was taken. The cell was outgassed from room temperature up to 200 °C and spectra were collected after each evacuation. All spectra were normalized to wafers weighing 15 mg.

2.3. Catalytic experiments

A glass batch reactor jacketed in a thermostatically controlled water bath, fitted with a condenser, mechanical stirrer and a thermocouple were used to carry out the oxidation reaction. In a typical run, the mixture containing 2196 S-ppm of dibenzothiophene (Aldrich, 98%) dissolved in acetonitrile (J.T. Baker, 99.99%) was added. When the desired temperature was reached and stabilized, the catalyst and H_2O_2 (PQF, 30% wt.) were introduced into the reactor with vigorous stirring, with an initial O/S molar ratio of 4.5. ODS reactions were carried out at 60 °C and atmospheric pressure. Reaction products were analyzed with an HP5890 Series II Gas Chromatograph with a PONA capillary column (Methyl silicone Gum, 50 m × 0.2 mm × 0.5 μm film thickness). Reactant and product identifications were performed by comparing retention times in GC-FID and, from results obtained with a GC-PFPD (Varian CP-3800) and GC–MS (HP5890 Series II with MS detector). H_2O_2 profiles were measured by standard iodometric titration.

3. Results and discussion

3.1. Catalyst characterization

Elemental analysis by SEM–EDX shows that the composition is similar to nominal contents presented in Table 1. Textural properties of the prepared catalysts by TS and IWI present a normal behavior as V is incorporated on the support (see Table 1), wherein surface area and pore volume decrease as V loading increases, while average pore is practically constant. But with SG method, V precursor was incorporated during preparation of the support, which permits to obtain a mixed oxide with small pores and higher surface area.

XRD results (Fig. 1) show that all catalysts prepared by thermal spreading present the main diffraction peaks attributable to crystalline V_2O_5, in $2\theta = 15°$, 20°, 22°, 26°, 31°, 32° and 34° [13]. While catalysts prepared by incipient wetness impregnation do not show any diffraction peak characteristic of V_2O_5 up to 15%, where the diffraction peak in $2\theta = 20°$ and 26° slightly appear. Catalysts prepared by sol–gel (not shown) did not show any crystalline phases. Raman spectroscopy under ambient conditions

Table 1
Textural properties of support and catalysts

	BET Area (m^2/g)	Pore volume (cm^3/g)	Average pore size (Å)	Surface density (V/nm^2)
Al_2O_3	206	0.39	76	–
5VATS	181	0.37	82	1.67
10VATS	171	0.35	81	3.28
15VATS	158	0.33	82	4.89
20VATS	147	0.3	82	6.50
5VAIWI	198	0.37	75	1.61
10VAIWI	180	0.33	74	3.21
15VAIWI	164	0.31	75	4.82
20VAIWI	150	0.28	76	6.43
8VASG	479	1.22	32	1.24[a]
15VASG	512	0.49	31	2.33[a]
26VASG	388	0.22	<26	4.03[a]

[a] Calculated from the V/Al molar ratio of the mixed oxide and the BET area of the alumina prepared by SG.

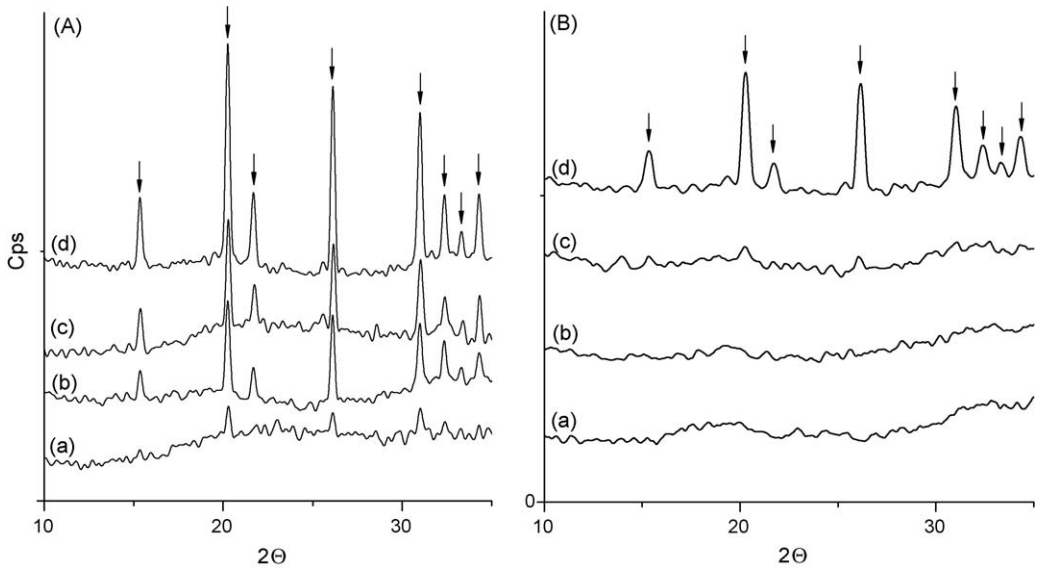

Fig. 1. XRD patterns of VO_x/Al_2O_3 catalysts prepared by (A) TS and (B) IWI, with (a) 5%, (b) 10%, (c) 15% and (d) 20% of V_2O_5.

confirmed this result by showing well-defined peaks of V_2O_5 localized at 993, 695, 515, 477, 403, 281 and 141 cm^{-1} in catalysts prepared by TS and 20VAIWI. 15VAIWI displays two broad peaks at 993 and 141 cm^{-1}. These peaks are indicative of microcrystalline V_2O_5 particles [14]. As observed by XRD, Raman spectra of sol–gel catalysts (Fig. 2) do not display any characteristic peak of crystalline V_2O_5. Only a broad peak around 925 cm^{-1} is observed, which increases intensity with vanadium loading. The broadness of this peak increases and a slight shoulder at 993 cm^{-1} is observed in 26VASG. This frequency matches with the main peak of V_2O_5 suggesting the presence of microcrystallites. A peak at ~940 cm^{-1} in VO_x/Al_2O_3 catalysts has been previously assigned [14] to surface metavanadate species, $(VO_3)_n$. In order to clarify this assignment, the Raman spectrum of pure crystalline ammonium metavanadate was taken as reference and it displayed a sharp peak at ~920 cm^{-1} (Fig. 2) as well as other peaks at 896, 647, 495, 387, 321, 262 and 217 cm^{-1}. Thus, the peak at 920 cm^{-1} suggests the presence of polymeric metavanadate species. The spectrum of V_2O_5 is also shown in order to simplify the assignment.

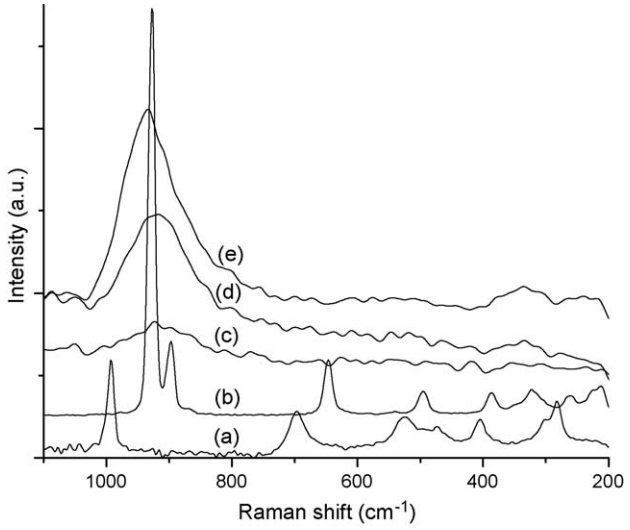

Fig. 2. Raman spectra under ambient conditions of: (a) crystalline V_2O_5, (b) crystalline NH_4VO_3, (c) 8VASG, (d) 15VASG and (e) 26VASG. (a) and (b) spectra were divided by a factor of 10.

Temperature-programmed reduction has provided very useful information on the nature and the strength of the interaction between supported species and support, and it has shown to be a sensitive technique for studying reducibility of V species [15]. Fig. 3 shows the TPR profiles of the catalysts. Thermal conductivity detector (TCD) signal of TPR experiments is calibrated by reduction of a high purity V_2O_5 sample, which is precisely the active phase of these catalysts and it was taken as reference. Bulk V_2O_5 exhibits a well-defined reduction peak from 450 to 850 °C, with temperature of reduction rate maximum (T_{max}) at 645 °C [11]. This peak is associated to the reduction of V(+5) to V(+3) species [15]. Supported vanadium oxide catalysts present similar reduction profiles at lower temperatures [12]. In this work, reduction peaks of alumina-supported vanadium oxide prepared by different methods start between 300 and 400 °C. These temperature shifts can be attributed to the presence of more easily reducible highly dispersed V species on the surface. TPR quantitative results show that the reduction degree is very high in the catalysts prepared by TS and IWI (more than 80%) and it depends on the V loading. In general, if V loading increases T_{max} increases and two reducible species are observed. At low surface coverage ($\upsilon < 15\%$) a shoulder or small peak at $T < 600$ °C was obtained, which could be attributed to monomeric and polymeric VO_4 units on the surface. At higher V content, the monolayer surface coverage was exceeded and V species were segregated showing a reduction peak at higher temperature.

The reduction degree and T_{max} of catalysts with the same V loading, prepared by TS or IWI method, were similar. But catalysts prepared by SG method present higher T_{max} and lower reduction degree going from 41% for 8VASG to 73% for 26VASG. This result suggests a strong V species-support interaction, which is expected with this kind of preparation. Reducibility trend obtained for the catalysts with similar vanadium content was: 15VAIWI (88.5% and T_{max} = 558 °C) > 15VATS (79.7% and 614 °C) > 15VASG (51.8% and 608 °C).

In order to obtain information about V species coordination UV–vis DRS was performed. Electronic spectra of reference V^{5+} compounds are shown in Fig. 4. V_2O_5 is known to have a distorted octahedral coordination while chains of corner shared tetrahedral vanadate units compose ammonium metavanadate. From this figure, differences in band maxima and edge energy of these two compounds are clearly observed. Electronic spectra of catalysts

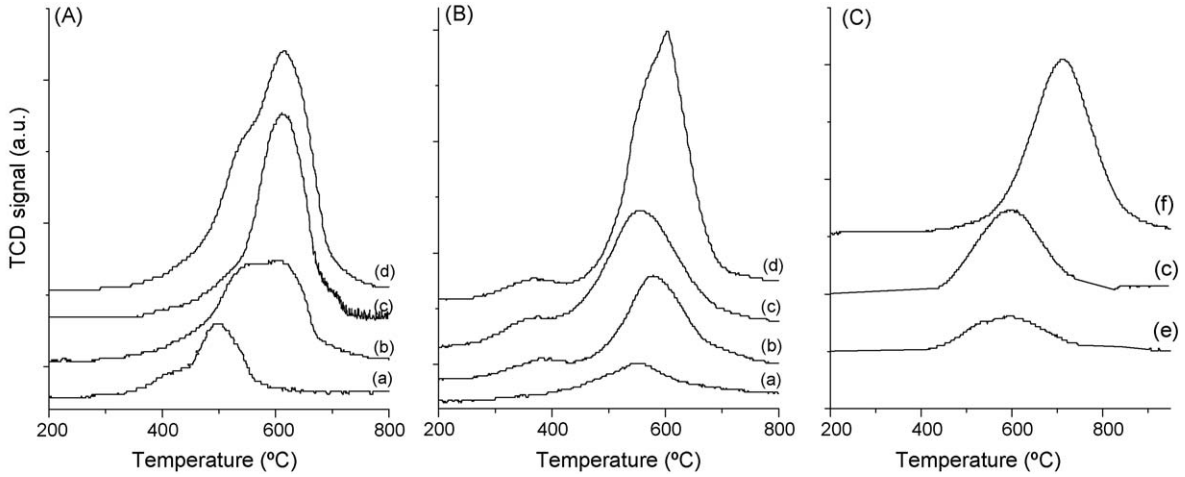

Fig. 3. TPR profiles of VO_x/Al_2O_3 prepared by (A) TS, (B) IWI and (C) SG, with (a) 5%, (b) 10%, (c) 15%, (d) 20%, (e) 8% and (f) 26% of V_2O_5.

prepared by TS and IWI are presented in Fig. 5. These catalysts show a ligand to metal charge transfer (LMCT) band at 250–260 nm due to electronic transitions of $O^{2-} \rightarrow V^{5+}$ which can be assigned to tetrahedral V^{5+} species [16–18]. These bands are not all quite symmetrical and the region at higher wavelength becomes broader as V loading increases up to a point where two bands are clearly observed. The first band maxima shift to lower wavelength and the second band is centered at ~303 nm on catalysts with the highest loading. It has been reported [19] that the band maximum of the CT transitions of V^{5+} shifts to higher energy (lower wavelength) with decreasing coordination number and that the polymerization of tetrahedral V^{5+} is only evidenced by a broadening of the absorption bands and/or a small shift of the absorption maxima to lower energy (higher wavelength). These results indicate that these catalysts present a highly heterogeneous surface composed of tetrahedral vanadate species and possibly segregated octahedral V_2O_5-like species. It is also observed that all catalysts prepared by TS display a slight tail extending beyond 540 nm, which increases intensity with vanadium loading. This absorption can also be assigned to V_2O_5 crystallites, as observed by XRD, with higher coordination (VO_5, VO_6).

Fig. 6 shows DRS spectra of sol–gel catalysts, which display two absorption bands at 218 and 268 nm. These bands change intensity with increasing vanadium loading and move towards higher wavelengths as it is observed with the first band of 26VASG, which reaches 238 nm. The bands resemble those of NH_4VO_3 that consists of chains of tetrahedral vanadate units; such a similarity was also observed by Raman spectroscopy. It is interesting to note that their edge energies are the highest of all catalysts prepared in this study, going from ~4 eV for 8VASG to 3.62 eV for 26VASG. No bands are observed due to d–d transitions of V^{4+}/V^{3+} metal cations (not shown), which occur as weak broad bands in the visible region (10,000–30,000 cm^{-1}) [19,20].

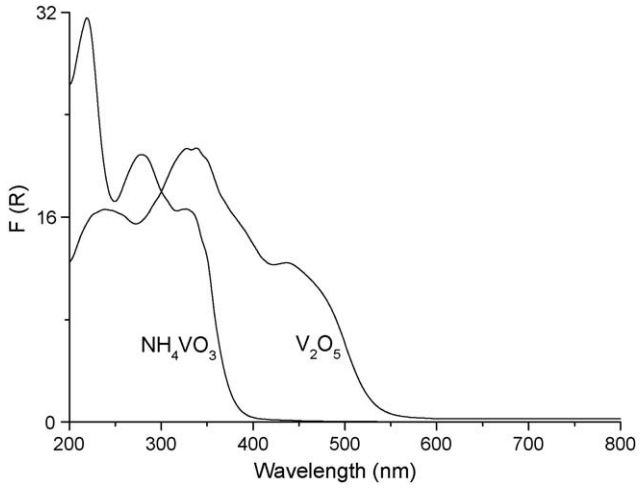

Fig. 4. UV–vis spectra of reference V^{5+} compounds.

IR spectra of adsorbed pivalonitrile (PN) on selected VO_x/Al_2O_3 catalysts were taken in order to evaluate Lewis acidity. PN is a weak base, and its IR spectrum is characterized by a strong band observed in the liquid at 2235 cm^{-1}, due to the stretching vibration mode of the C≡N triple bond. This band shifts to higher frequency when PN interacts with electron withdrawing centers through its nitrogen lone pair [21]. Fig. 7 shows the IR subtraction spectra of adsorbed PN on VO_x/Al_2O_3. Two well-defined bands with maxima at ~2294 and ~2245 cm^{-1} are observed. According to the literature [22] these bands have been assigned to PN coordinated (high frequency, HF) and hydrogen bonded to OH's groups (low frequency, LF). When outgassing temperature is increased, the IR bands intensity decreases, being this effect more pronounced for VASG catalysts. After evacuation at 100 °C, shoulders at ~2273 and ~2240 cm^{-1} are observed, their assignment will be discussed later. It is also evident that the ratio between HF and LF band intensities changes with the catalysts preparation method and with V loading, especially for VATS and VASG catalysts. This behavior could be attributed to a higher amount of hydroxyl groups on the surface coming either from alumina support due to vanadium segregation or by polymerization of surface VO_x species when V loading is increased from 5 to 15%.

The fundamental region in the subtraction spectra after PN adsorption (not shown) shows a negative band at ~1030 cm^{-1}, characteristic of stretching vibration mode of terminal V=O groups whose intensity decreases (as the band assigned to coordinated PN) and shifts to higher wavenumbers with outgassing temperature. This means that the intensity of the band assigned to Lewis acidic sites must have the contribution of V^{5+} and Al^{3+} CUS.

Al_2O_3 and V_2O_5 are known to possess Lewis acid sites and their corresponding vibration frequencies with adsorbed PN are 2295 and 2280 cm^{-1}, respectively [22]. Subtraction IR Al_2O_3 spectra obtained after PN adsorption (Fig. 8) show indeed a broad peak at 2295 cm^{-1} also composed by a shoulder at 2273 cm^{-1}. This can be assigned to the presence of two types of Al^{3+} coordinative unsaturated sites. In an attempt to distinguish between Lewis acid sites corresponding to vanadium and those of support,

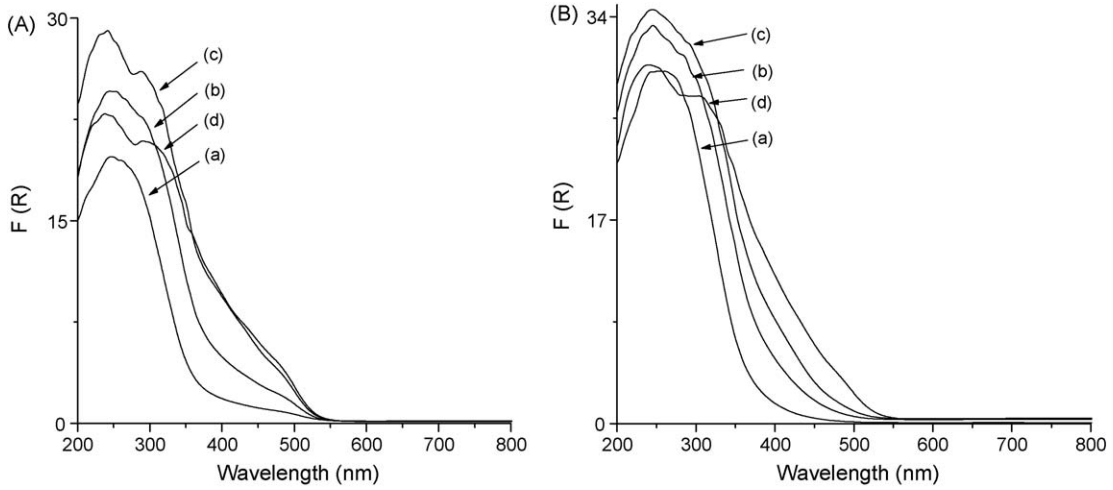

Fig. 5. UV–vis spectra of VO_x/Al_2O_3 prepared by (A) TS and (B) IWI, with (a) 5%, (b) 10%, (c) 15% and (d) 20% of V_2O_5.

deconvolution of IR bands was made. The ratio of Lewis acid sites corresponding to Al (LAl) and V (LV) are presented in Table 2. It can be observed that LAl/LV ratio of TS and IWI catalysts decreases with increasing vanadium loading, which might be due to a higher amount of vanadium species that chemisorbs PN at coordinative unsaturated sites or defect sites. It is also observed that LAl/LV ratio of not well-dispersed 5VATS is higher than well-dispersed 5VAIWI. This indicates that for the later, a higher amount of LV sites is "available". Sol–gel catalysts do not show the trend observed with TS and IWI. The IR bands for these mixed oxides presented the lowest IR intensity indicating poor accessibility for PN adsorption. IR spectrum of adsorbed PN on 26VASG (not shown) displayed practically no Lewis acidity. In summary, these catalysts characterizations show that the preparation method does affect V dispersion. Surface V oxide species are known to be independent on preparation method, when calcined during long time at higher temperatures than Tamman [23]. However, as stated above, the amount of each type of V species can be varied with the preparation method.

3.2. Oxidative desulfurization

Liquid phase oxidation of dibenzothiophene with H_2O_2 was carried out in presence of VO_x/Al_2O_3 as catalysts and acetonitrile as

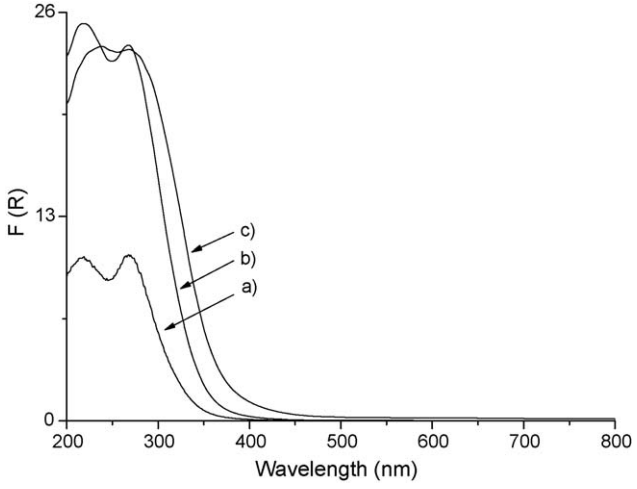

Fig. 6. UV–vis spectra of VO_x/Al_2O_3 prepared by SG, with (a) 8%, (b) 15% and (c) 26% of V_2O_5.

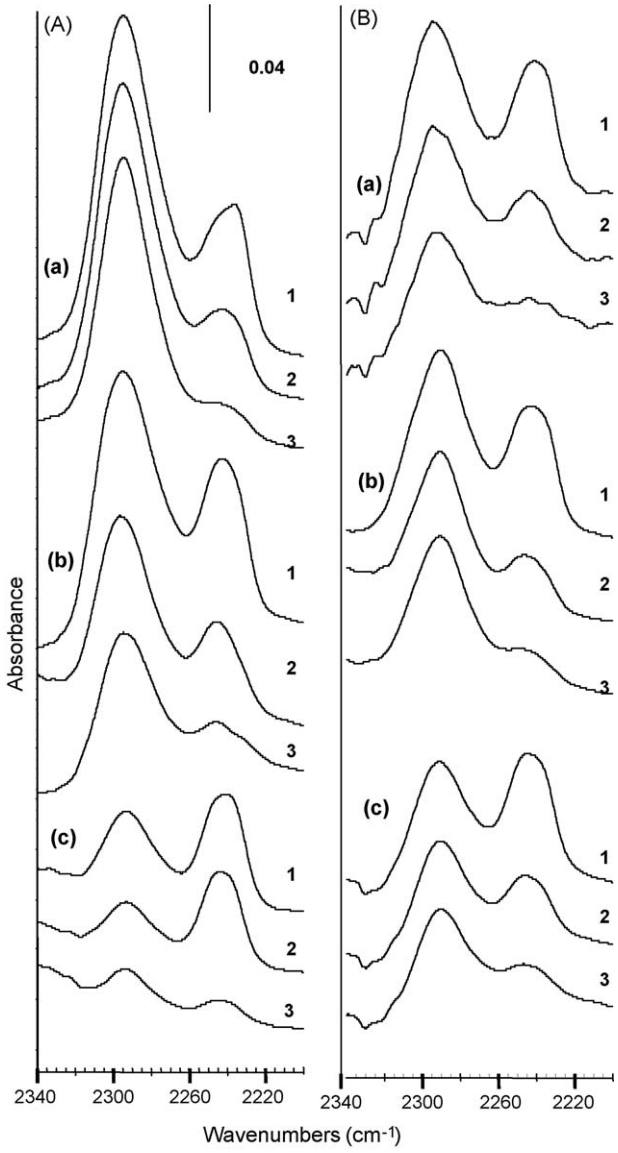

Fig. 7. IR subtraction spectra of evacuated PN at: (1) room temperature, (2) 50 °C and (3) 100 °C on VO_x/Al_2O_3. (A) Low loadings: (a) 5VATS, (b) 5VAIWI and (c) 8VASG. (B) High loadings: (a) 15VATS, (b) 15VAIWI and (c) 15VASG.

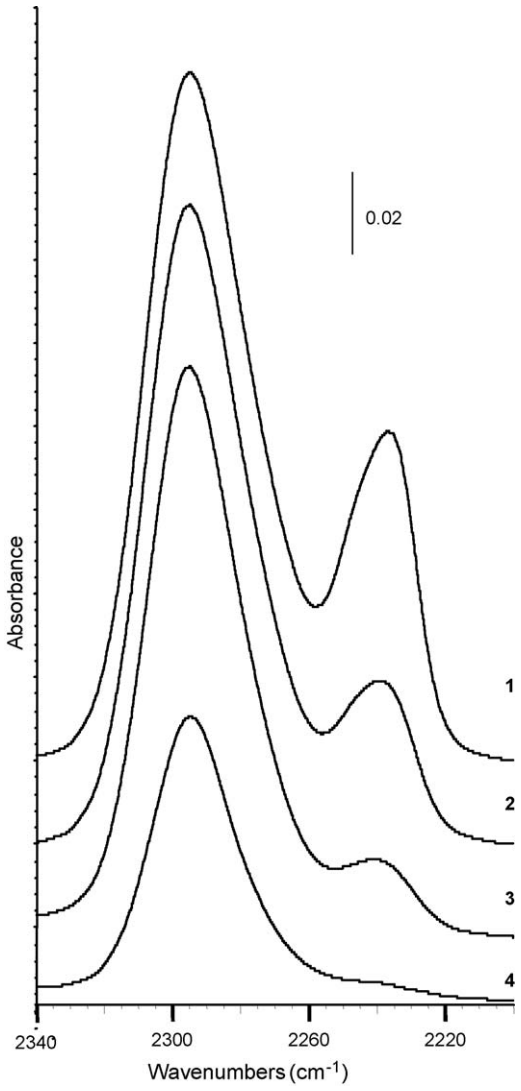

Fig. 8. IR subtraction spectra of evacuated PN on Al_2O_3 at: (1) room temperature, (2) 50 °C, (3) 100 °C and (4) 200 °C.

solvent. Full oxidation of dibenzothiophene was often reached, which results in high yield to dibenzothiophene sulfone (DBTDO) and practically no DBT sulfoxide. Activity results after 30 min of reaction with all catalysts, expressed as V/nm^2, are shown in Fig. 9. It can be observed that catalysts prepared by TS present higher activity at lower loadings than the ones prepared by IWI. The latter catalysts show a clearer increase in activity as V loading increases up to the monolayer, where the V_2O_5 phase begins to appear. Sol–gel catalysts have low oxidation activity and it decreases with

Table 2
H_2O_2 remaining after 30 min of reaction and Lewis acidity ratio

V_2O_5 (wt.%)	TS catalyst		IWI catalyst		SG catalyst	
	H_2O_2 (%)	LAl/LV[a]	H_2O_2 (%)	LAl/LV	H_2O_2 (%)	LAl/LV
5	36.6	5.2	69.5	2.9	–	–
10	1.0	n.d.	3.7	n.d.	91.5[b]	1.9[b]
15	1.0	3.1	1.2	2.5	85.4	3.4
20	1.0	n.d.	1.2	n.d.	82.9[c]	n.d.

[a] LAl/LV ratios calculated from the area under the curve of each IR band.
[b] 8% of V_2O_5.
[c] 26% of V_2O_5. n.d.: not determined.

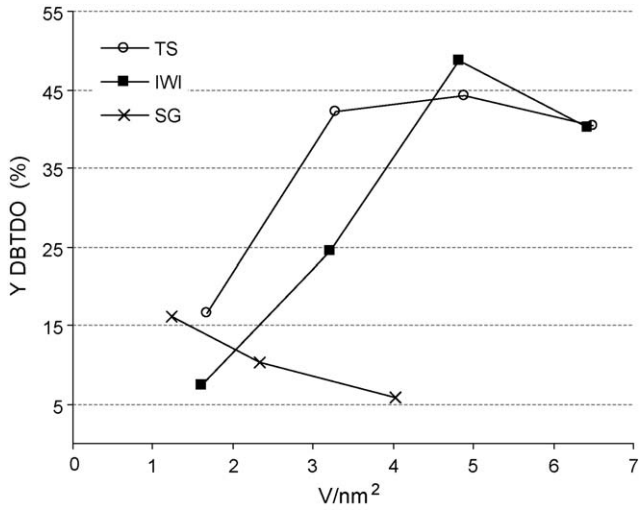

Fig. 9. DBT sulfone yield (after 30 min of reaction) in function of V surface density, for TS, IWI and SG catalysts.

increasing vanadium loading. It was stated in the previous section that all TS preparations presented V_2O_5 crystallites, while IWI catalysts presented better dispersed V species and V_2O_5 crystallites begin to appear with 15% of V_2O_5. This fact suggests that V_2O_5 crystallites increase activity at low V loadings up to a point where bigger V clusters are formed and V "accessibility" is lowered. Sol–gel catalysts did not display evident crystalline phases, and correlations between V species and performance are not straightforward in this case. IR spectra of adsorbed PN on these catalysts exhibit low Lewis acidity and it seems to decrease with increasing vanadium loading, although 15VASG does not follow this trend. H_2O_2 profiles were monitored in every reaction test and no clear changes in the percentage of H_2O_2 remaining after reaction were observed with TS and IWI (Table 2). Reducibility of these catalysts is over 80%, as observed by TPR, and it follows no trend either, which explains the low amounts of H_2O_2 after reaction in these cases. H_2O_2 titrations with sol–gel catalysts demonstrate that peroxide is not decomposed, since more than 80% of the oxidant remains in the system after reaction time (Table 2). Reducibility of these catalysts was rather low and it increases with vanadium loading, this is in agreement with the percentages of H_2O_2 shown in Table 2.

As liquid phase reactions catalyzed by solids are known to involve leaching of the active phase [24,25], heterogeneity tests of some IWI catalysts were performed. These tests consisted in filtering the catalyst after 10 min of reaction at the same reaction temperature, then the filtrate is introduced into the reactor, and the homogeneous reaction is carried out. It was observed that partially homogenous reaction was taking place with 15VAIWI (4.8 V/nm^2) while 5VAIWI (1.6 V/nm^2) presented heterogeneous activity without leaching, as it can be observed in Fig. 10. This might be due to the presence of "three legged" monovanadate species at such low vanadium loading [26], which agrees with the result obtained by TPR that shows only one reduction peak. Also, the final solution of the liquid phase oxidation of DBT (when using 5VAIWI) did not show any color indicative of leached V, as most of the solutions of the other catalysts did, except 8VASG and 15VASG. All catalysts prepared by TS undergo leaching of vanadium due to poor stability of V_2O_5 crystallites and surface polyvanadates in presence of polar molecules. Thus, it is believed that such higher activities obtained with low V loadings are due to homogenous activity of leached vanadium.

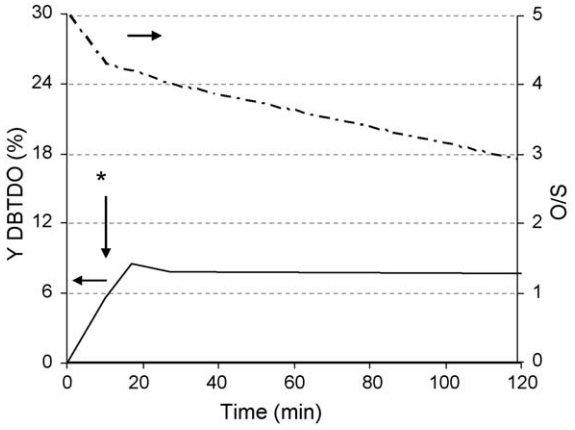

Fig. 10. Heterogeneity test of 5VAIWI. Straight line corresponds to sulfone profile and dashed line to H_2O_2 profile. (*) Catalyst withdrawal at 10 min.

As it was described elsewhere [12,25], these catalysts "activate" H_2O_2 by homolytic or heterolytic routes. In homolytic routes transition metals catalyze the free radical autoxidation process and undergo a change in oxidation state. Heterolytic routes involve complex formation of oxometal and peroxometal kind, where only the former undergoes a redox process. V^{5+} should typically follow the peroxometal route when catalyzing heteroatom oxidations, acting as a Lewis acid to render the peroxidic bond more reactive. There lies the importance of discerning between Lewis acid sites corresponding to alumina (LAl) and vanadium (LV), given that coordinative unsaturated vanadium species will most likely be able to form the oxidant peroxocomplex. It has been reported by Martínez-Huerta et al. [27] that monomeric vanadium species possess stronger Lewis acidity than polymerized species, but with our catalytic tests no comparisons can yet be made regarding this topic because more polymerized species presented leaching of the active phase, and catalytic activity in those cases could have involved homogeneous and heterogeneous contributions.

Vanadium species in sol–gel catalysts have shown to have a strong interaction with alumina as observed by their low reducibility in TPR. With these catalysts the amount of H_2O_2 in the system after reaction decreased with increasing reducibility (see Fig. 3 and Table 2), which suggests that OH^* radicals formed after H_2O_2 homolytic decomposition are not responsible of dibenzothiophene oxidation, since more reducible 26VASG presented the lowest activity. Hence, according to these results the vanadium peroxocomplex is the oxidant species responsible of dibenzothiophene oxidation. It was also observed that 8VASG seems to activate H_2O_2 more selectively as a high percentage of peroxide remains in the system after reaction and its activity is higher than that of 5VAIWI.

4. Conclusions

High liquid phase DBT oxidation activities were obtained with VO_x/Al_2O_3 prepared by TS and IWI methods. Catalysts prepared by IWI resulted in better dispersed V species than TS. SG catalysts have a strong interaction with alumina, and ODS activity decrease with increasing V loading while their reducibility exhibits a reverse trend.

IWI method produced a higher amount of vanadium Lewis acidic sites compared with TS and SG methods according to PN adsorption results. Apparently the V Lewis acidic sites could be related to ODS activity.

Partially homogenous reaction was observed beyond 1.6 V/nm^2 with IWI and TS, which can be attributed to lower V–O–Al interaction of polymerized V species and V_2O_5 crystallites, while monovanadates have higher interaction with the support due to their three V–O–Al bonds. The proposed reaction pathway is the peroxocomplex formation as oxidant species since it does not involve a change in oxidation state of the metal.

Acknowledgements

This work was supported by DGAPA-UNAM (IN102408 Project). H. Gomez acknowledges CONACyT for her scholarship. Technical assistance of I. Puente (SEM–EDX), R. Sato (Raman) and C. Salcedo (XRD) is gratefully acknowledged.

References

[1] I.V. Babich, J.A. Moulijn, Fuel 82 (2003) 607.
[2] C. Song, Catal. Today 86 (2003) 211.
[3] E. Ito, J.A. Rob van Veen, Catal. Today 116 (2006) 446.
[4] Y. Shiraishi, T. Hirai, Energy Fuels 18 (2004) 37.
[5] T. Aida, D. Yamamoto, M. Iwata, K. Sakata, Rev. Heteroatom. Chem. 22 (2000) 241.
[6] A. Ishihara, D. Wang, F. Dumeignil, H. Amano, E.W. Qian, T. Kabe, Appl. Catal. A 279 (2005) 279.
[7] V. Hulea, F. Fajula, J. Bousquet, J. Catal. 198 (2001) 179.
[8] S. Murata, K. Murata, K. Kidena, M. Nomura, Energy Fuels 18 (2004) 116.
[9] D. Wang, E.W. Qian, H. Amano, K. Okata, A. Ishihara, T. Kabe, Appl. Catal. A 253 (2003) 91.
[10] H. Gomez, L. Cedeño, Int. J. Chem. Reactor Eng. 3 (2005) A28. www.bepress.com/ijcre/vol3/A28.
[11] L. Cedeño-Caero, J. Navarro, A. Gutierrez-Alejandre, Catal. Today 116 (2006) 562.
[12] L. Cedeño, H. Gomez-Bernal, A. Fraustro-Cuevas, H.D. Guerra-Gomez, R. Cuevas-Garcia, Catal. Today 133–135 (2008) 244.
[13] ASTM Powder Diffraction File 9-387, Ed. Joint Committee on Powder Diffraction Standards, Pennsylvania, 1979.
[14] G. Deo, I.E. Wachs, J. Phys. Chem. 95 (1991) 5889.
[15] I.E. Wachs, Y. Chen, J. Jehng, L.E. Briand, T. Tanaka, Catal. Today 78 (2003) 13.
[16] M.A. Larrubia, G. Busca, Mater. Chem. Phys. 72 (2001) 337.
[17] J.G. Eon, R. Olier, J.C. Volta, J. Catal. 145 (1994) 318.
[18] P. Concepción, M.T. Navarro, T. Blasco, J.M. López Nieto, B. Panzacchi, F. Rey, Catal. Today 96 (2004) 179.
[19] G. Catana, R. Ramachandra Rao, B.M. Weckhuysen, P. Van Der Voort, E. Vansant, R.A. Schoonheydt, J. Phys. Chem. B 102 (1998) 8005.
[20] L.J. Burcham, G. Deo, X. Gao, I.E. Wachs, Top. Catal. 11/12 (2000) 85.
[21] A. Gutiérrez-Alejandre, M. Trombetta, G. Busca, J. Ramírez, Micropor. Mater. 12 (1997) 79.
[22] G. Busca, Catal. Today 41 (1998) 191.
[23] B.M. Weckhuysen, D. Keller, Catal. Today 78 (2003) 25.
[24] R.A. Sheldon, M. Wallau, I.W.C.E. Arends, U. Schuchardt, Acc. Chem. Res. 31 (1998) 485.
[25] I.W.C.E. Arends, R.A. Sheldon, Appl. Catal. A 212 (2001) 175.
[26] H. Tian, E.I. Ross, I. Wachs, J. Phys. Chem. B 110 (2006) 9593.
[27] M.V. Martínez-Huerta, X. Gao, H. Tian, I.E. Wachs, J.L.G. Fierro, M.A. Bañares, Catal. Today 118 (2006) 279.